ORIGINAL RESEARCH

Translocase of Inner Membrane 50 Functions as a Novel Protective Regulator of Pathological Cardiac Hypertrophy

Kai Tang, MD;* Yifan Zhao, MD;* Hailing Li, MD; Mengyun Zhu, MD; Weiming Li, MD; Weijing Liu, MD; Guofu Zhu, MD; Dachun Xu, MD; Wenhui Peng, MD, PhD; Ya-wei Xu, MD, PhD, FACC

***Background*—**Translocase of inner membrane 50 (TIM50) is a member of the translocase of inner membrane (TIM) complex in the mitochondria. Previous research has demonstrated the role of TIM50 in the regulation of oxidative stress and cardiac morphology. However, the role of TIM50 in pathological cardiac hypertrophy remains unknown.

***Methods and Results*—**In the present study we found that the expression of TIM50 was downregulated in hypertrophic hearts. Using genetic loss-of-function animal models, we demonstrated that TIM50 deficiency increased heart and cardiomyocyte size with more severe cardiac fibrosis compared with wild-type littermates. Moreover, we generated cardiomyocyte-specific TIM50 transgenic mice in which the hypertrophic and fibrotic phenotypes were all alleviated. Next, we tested reactive oxygen species generation and the activities of the antioxidant enzymes superoxide dismutase and catalase, and also respiratory chain complexes I, II, and IV, finding that all the activities were regulated by TIM50. Meanwhile, expression of the ASK1-JNK/P38 axis was increased in TIM50-deficient mice, and TIM50 overexpression decreased the activity of the ASK1-JNK/P38 axis. Finally, we treated mice with the antioxidant N-acetyl cysteine to reduce oxidative stress. After N-acetyl cysteine treatment, the deteriorative hypertrophic and fibrotic phenotypes caused by TIM50 deficiency were all remarkably reversed.

***Conclusions*—**These data indicated that TIM50 could attenuate pathological cardiac hypertrophy primarily by reducing oxidative stress. TIM50 could be a promising target for the prevention and therapy of cardiac hypertrophy and heart failure. **(*J Am Heart Assoc*. 2017;6:e004346. DOI: 10.1161/JAHA.116.004346.)**

Key Words: cardiac hypertrophy • heart failure • mitochondrial • oxidative stress • TAK1-JNK/P38 • translocase of inner membrane 50

Pathological cardiac hypertrophy, which is commonly seen in hypertension, ischemia, and valvular heart disease,[1] is a complex and dynamic process that occurs during long-standing pressure or volume overload. Various intracellular mechanisms are involved in the regulation of cardiac hypertrophy.[2] Among them, oxidative stress is considered closely related to pathological cardiac hypertrophy.[3] In the physiological state ion leakage from oxidative phosphorylation (OXPHOS) may generate some reactive oxygen species[4] (ROS), which can be eliminated by ROS scavenger enzymes such as superoxide dismutase (SOD) and catalase,[5] maintaining a stable status in the body. In some pathological conditionsS the balance between ROS generation and elimination is disrupted, thus leading to excessive oxidative stress.[6,7] Numerous researches have observed that oxidative stress has a close relationship with pathological cardiac hypertrophy,[8-10] and many mitochondrial proteins can regulate the extent of oxidative stress during the process of cardiac hypertrophy.[11,12] Therefore, proteins that selectively regulate oxidative stress may possess a potential therapeutic function in pathological cardiac hypertrophy.

Mitochondria contain ~1000 different proteins, but only 13 of these proteins are encoded by the mitochondrial genome and are synthesized in the matrix.[13] Therefore, ~99% of the mitochondrial proteins must be transported from the cytosol to the mitochondrial membrane or matrix.[14] These mitochondrial proteins are recognized by the translocase in the mitochondrial membrane. There are 3 well-characterized mitochondrial translocase complexes: 1 translocase of outer

From the Department of Cardiology, Shanghai Tenth People's Hospital, Tongji University School of Medicine, Shanghai, China.

Accompanying Figures S1 through S3 are available at http://jaha.ahajournals.org/content/6/4/e004346/DC1/embed/inline-supplementary-material-1.pdf

*Dr Tang and Dr Zhao contributed equally to this work.

Correspondence to: Wenhui Peng, MD, PhD, or Ya-wei Xu, MD, PhD, FACC, Department of Cardiology, Shanghai Tenth People's Hospital, Tongji University School of Medicine, 301 Yanchang Middle Road, Shanghai 200072, China. E-mail: pwenhui@tongji.edu.cn, xuyawei@tongji.edu.cn

Received August 18, 2016; accepted February 15, 2017.

membrane (TOM) complex, the TOM40 complex; and 2 translocase of inner membrane (TIM) complexes, the TIM22 and TIM23 complexes. TIM22 and TIM23 recognize different types of mitochondrial proteins.[14] Some members of the translocase complex have been shown to be associated with human disease including heart disease.[15-17]

TIM50 is a member of the TIM23 complex that functions as a receptor for presequence-carrying proteins.[18] Under physiological conditions, TIM50 is essential for directing mitochondrial matrix proteins to the import channel of the TIM23 complex[19] and maintaining the permeability barrier of the mitochondrial inner membrane.[20] The depletion of TIM50 in zebra fish leads to the disorganization and truncation of skeletal muscle fibers as well as to cardiac dilatation.[21] This result raises the possibility that TIM50 may regulate cardiac remodeling and heart failure. However, there is still no direct evidence that TIM50 is involved in cardiac remodeling. Thus, our aim is to fully elucidate the role of TIM50 in the regulation of pathological cardiac remodeling.

In the present study we found that TIM50 was downregulated in both human dilated cardiomyopathy (DCM) hearts and hypertrophic murine hearts. Meanwhile, TIM50-deficient mice showed more severe cardiac hypertrophy than wild-type mice, whereas the cardiac-specific overexpression of TIM50 in mice demonstrated a protective effect. Similar results were shown in cultured neonatal rat cardiomyocytes with the gain or loss of function of TIM50. Furthermore, we observed that TIM50 regulated cardiac hypertrophy via reducing ROS accumulation and ASK1 activity. In general, we demonstrated for the first time that TIM50 is a novel negative regulator of pathological cardiac hypertrophy.

Methods and Materials

Experimental Design

We measured TIM50 expression level in human heart samples first. Then, we generated TIM50 global knockout mice and TIM50 cardiac-specific overexpression mice to figure out the function of TIM50 in cardiac hypertrophy. Cardiac hypertrophy and function were assessed by using echocardiography, histological analysis, Western blot, and real-time polymerase chain reaction (PCR). Furthermore, oxidative stress and related biological processes were analyzed to elucidate the underlying mechanism by which TIM50 regulates cardiac hypertrophy.

Reagents

Antibodies against the following proteins were purchased from Santa Cruz Biotechnology (Dallas, TX): ANP (sc20158 1:200), β-MHC (sc53090 1:200), TIM50 (sc55338 1:200), and ASK1 (sc7931, 1:200). The following antibodies were purchased from Cell Signaling Technology (Danvers, MA): GAPDH (#2118 1:1000), phospho-ASK1^{Thr845} (3765, 1:1000), phospho-MEK1/2$^{Ser217/221}$ (#9154 1:1000), total-MEK1/2 (#9122 1:1000), phospho-ERK1/2Thr$^{202/204}$ (#4370 1:1000), total-ERK1/2 (#4695 1:1000), phospho-JNK1/2$^{Thr183/Tyr185}$ (#4668 1:1000), total-JNK1/2 (#9258 1:1000), phospho-P38$^{Thr180/182}$ (#4511 1:1000), and total-P38 (#9212 1:1000). Drp1 (#184272, 1:500), Mfn1 (#57602, 1:500), Mfn2 (#56889, 1:500) and Nrf2 (#31163, 1:500) were purchased from Abcam (Cambridge, MA), Fetal calf serum was purchased from HyClone (Waltham, MA). The other reagents for cell culture were purchased from Sigma (St. Louis, MO).

Human Heart Samples

All the procedures involving human heart samples followed the principle outlined in the Declaration of Helsinki and were approved by the Ethics Committee at Tongji University. Failing human hearts were obtained from the dilated cardiomyopathy patients who underwent heart transplantation (n=6). The control samples were obtained from heart donors who died in a car accident or due to severe traumatic brain injury and were unsuitable for heart transplantation for technical reasons (n=6). Written informed consent was obtained from each DCM patient and from the relatives of the heart donors.

Experimental Mouse Models

All the animal procedures were performed to conform to the NIH guidelines (Guide for the Care and Use of Laboratory Animals) and approved by the Animal Care and Use Committees of Shanghai Tenth People's Hospital.

Generation of Global TIM50 Knockout Mice

The global TIM50 knockout mice were generated using the CRISPR-Cas9 technique. The online CRISPR design tool (http://crispr.mit.edu) was used to predict the guide sequences of the target site for the mouse TIM50 gene. Then a pair of oligomers (oligo1: TAGGCCTTGGAGCCCCCACGGT and oligo2: AAAC ACCGTGGGGGCTCCAAGG) were annealed and cloned in the pUC57-sgRNA expression vector (Addgene, Cambridge, MA; 51132). sgRNA and Cas9 were then transcribed using the MEGAshortscript Kit (Ambion, Thermo Fisher Scientific, Waltham, MA; AM1354) and a T7 Ultra Kit (Ambion, Am1345), respectively. Cas9 and sgRNA mRNA were injected into single-cell embryos using a microinjection system (FemtoJet 5247, Eppendorf, Hamburg, Germany). PCR analysis (primers TIM50-238-F [5′-CTGGATGTC CACTTCCTGGT-3′] and TIM50-238-R [5′-CTGACAGTCCCA

CCAGCTC-3′]) was used to detect F1 and F2 offspring. The wild-type allele contained a 238-bp amplicon, and the mutant allele contained a 216-bp amplicon. Finally, Western blot analysis was used to further confirm the expression of TIM50 in mouse hearts.

Generation of Cardiac-Specific TIM50 Transgenic Mice

To generate TIM50 cardiac-specific transgenic mice (C57BL/6J background), we generated a pCAG-loxP-CAT-loxP-TIM50-polyA construct. The plasmid containing this construct was microinjected into fertilized murine embryos to obtain the transgenic mice. To induce cardiomyocyte-specific TIM50 expression, the CAG-CAT-TIM50-A transgenic mice were crossed with transgenic mice that carried the *Cre* gene under control of the α-MHC gene promoter. *Cre*-mediated recombination of floxed alleles was induced by daily intraperitoneal injection of 80 mg/kg of an emulsion containing 200 mg of tamoxifen (Sigma, T-5648) dissolved in 1 mL of ethanol, and 3 mL was then added to 9 mL of corn oil (Sigma, C-8267) to attain a final tamoxifen concentration of 20 mg/mL for 5 consecutive days. Four independent transgenic lines were successfully generated. Finally, the protein level of TIM50 in each line was detected by Western blotting.

Animal Surgery (Aortic Banding)

The surgical procedure was previously described elsewhere.[22,23] In brief, 8- to 10-week-old male mice were anesthetized with pentobarbital sodium (50 mg/kg intraperitoneally [ip]; Sigma, St. Louis, MO). Then the left chest of each mouse was opened. A 27-gauge needle was ligated together with the descending aorta (thoracic aorta) by 7-0 silk sutures to form an ~70% aortic constriction. The needle was removed, and the thoracic cavity was then closed. Sham-operated animals underwent the same surgical procedure without partial aortic ligation. At the indicated time points (4 and 8 weeks after aortic banding [AB] or sham operation), the mouse hearts, lungs, and tibia were collected and weighed. Then, 5- to 6-week-old mice were fed with N-acetyl cysteine (NAC, 500 mg/kg per day in drinking water, Sigma-Aldrich, St. Louis, MO) until the AB operation. The same volume of phosphate-buffered saline (PBS) was used as the control agent.

Mouse Grouping

Mouse models were divided into 8 groups: wild-type sham (n=12), TIM50-KO sham (n=12), wild-type AB (n=12), TIM50-KO AB (n=12), control littermates (CTMC) sham (n=12), TIM50-transgenic (TG) sham (n=12), CTMC AB (n=12), TIM50-TG AB (n=12).

Table 1. Primers for Real-Time PCR

Gene Name	Primer	Sequence
ANP-Rat	Forward 5′-3′	AAAGCAAACTGAGGGCTCTGCTCG
	Reverse 5′-3′	TTCGGTACCGGAAGCTGTTGCA
BNP-Rat	Forward 5′-3′	CAGCAGCTTCTGCATCGTGGAT
	Reverse 5′-3′	TTCCTTAATCTGTCGCCGCTGG
α-MHC-Rat	Forward 5′-3′	GCTCCAGGGGTGATGGACAA
	Reverse 5′-3′	GATTCGATACCTCTGCCGGA
β-MHC-Rat	Forward 5′-3′	TCTGGACAGCTCCCCATTCT
	Reverse 5′-3′	CAAGGCTAACCTGGAGAAGATG
ANP-Mouse	Forward 5′-3′	ACCTGCTAGACCACCTGGAG
	Reverse 5′-3′	CCTTGGCTGTTATCTTCGGTACCGG
BNP-Mouse	Forward 5′-3′	GAGGTCACTCCTATCCTCTGG
	Reverse 5′-3′	GCCATTTCCTCCGACTTTTCTC
β-MHC-Mouse	Forward 5′-3′	CCGAGTCCCAGGTCAACAA
	Reverse 5′-3′	CTTCACGGGCACCCTTGGA
Collagen I-Mouse	Forward 5′-3′	AGGCTTCAGTGGTTTGGATG
	Reverse 5′-3′	CACCAACAGCACCATCGTTA
Collagen III-Mouse	Forward 5′-3′	CCCAACCCAGAGATCCCATT
	Reverse 5′-3′	GAAGCACAGGAGCAGGTGTAGA
CTGF-Mouse	Forward 5′-3′	TGACCCCTGCGACCCACA
	Reverse 5′-3′	TACACCGACCCACCGAAGACACAG
TIM50-Rat	Forward 5′-3′	AGTCGTGGACTGCAAGAAGG
	Reverse 5′-3′	TGCTGCTCCTCCTGTTCAAG

ANP indicates atrial natriuretic peptide; BNP, brain natriuretic peptide; CTGF, connective tissue growth factor; α-MHC, α-myosin heavy chain; PCR, polymerase chain reaction; TIM50, translocase of inner membrane 50.

Echocardiography

Echocardiography was performed with a Vevo2100 imaging system (VisualSonics Inc, Toronto, ON, Canada) with an MS-400 ultrasound transducer. After anesthetization (2% inhaled isoflurane), the left ventricles (LV) of the mice were assessed in both parasternal short-axis and long-axis view at a frame rate of 120 Hz. End systole and end diastole were respectively defined as the phases in which the smallest and largest LV area was obtained. The LV end-systolic diameter and LV end-diastolic diameter were measured from the LV M-mode tracing with a sweep speed of 50 mm/s at the mid–papillary muscle level.

Histological Analysis

Anesthetized mice (pentobarbital sodium, 50 mg/kg, ip) were sacrificed immediately after echocardiography and hemodynamic measurements. The hearts were excised and instantly placed in a 10% potassium chloride solution to ensure that they were arrested in diastole. Then the mouse hearts were

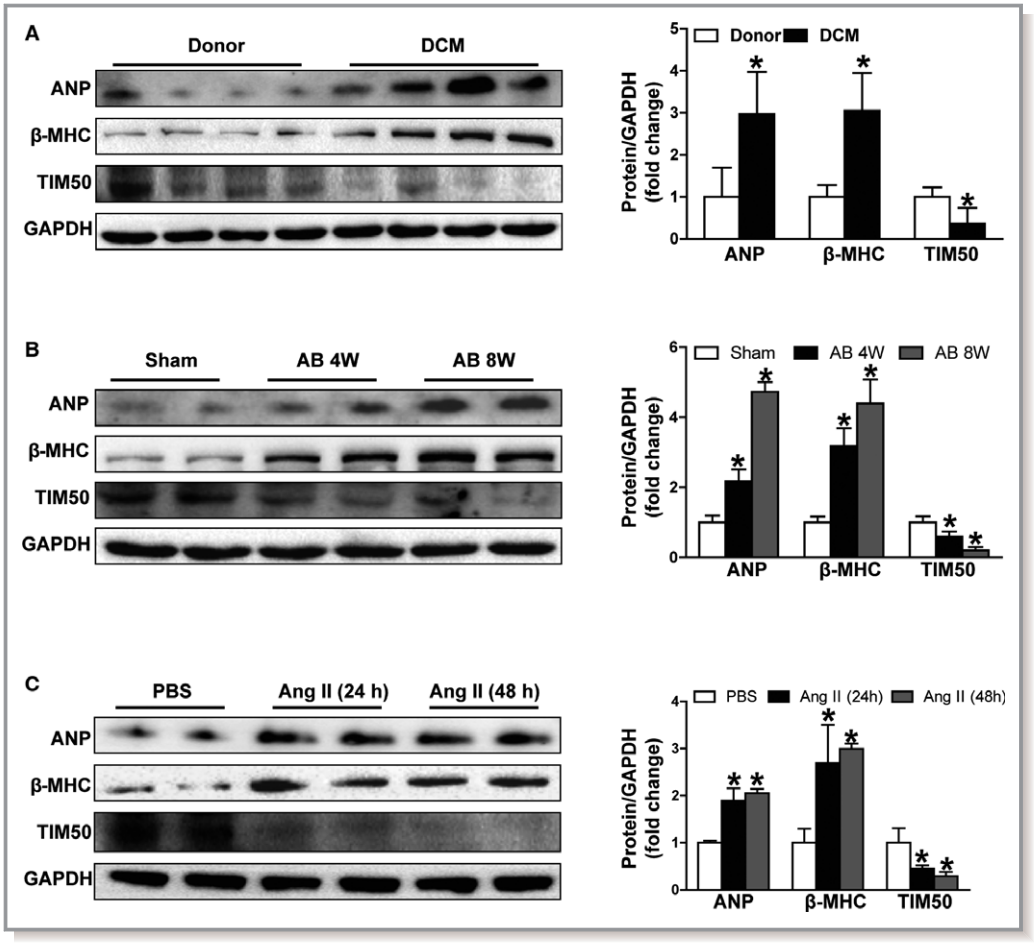

Figure 1. TIM50 expression is decreased in hypertrophic hearts and cardiomyocytes. A, Western blot analysis of ANP, β-MHC, and TIM50 in dilated cardiomyopathic hearts (n=6 for each experimental group, **P*<0.05 vs donor group). B, Western blot analysis of ANP, β-MHC and TIM50 in AB-induced hypertrophic hearts in mice (n=6 for each experimental group, **P*<0.05 vs sham group). C, Western blot analysis of ANP, β-MHC, and TIM50 in Ang II-induced hypertrophic cardiomyocytes (n=3 independent experiments, **P*<0.05 vs PBS group). All data are presented as mean±SD. AB indicates aortic banding; Ang II, angiotensin II; ANP, atrial natriuretic peptide; DCM, dilated cardiomyopathy; β-MHC, β-myosin heavy chain; PBS, phosphate-buffered saline; TIM50, translocase of inner membrane 50.

fixed with 10% formalin, dehydrated, and embedded in paraffin. Subsequently, the hearts were sectioned transversely close to the apex to visualize the left and right ventricles at 5 μm. Several sections of each heart were prepared and stained with hematoxylin-eosin (HE) or with picrosirius red following standard procedures to evaluate the cross-sectional area or collagen deposition, respectively, and then visualized using light microscopy. To further confirm the cell size observed by HE staining, heart sections were stained with fluorescein isothiocyanate–conjugated wheat germ agglutinin (WGA; Invitrogen, Carlsbad, CA) to visualize the membranes and with DAPI to observe the nuclei. After HE and picrosirius red staining, more than 100 LV myocytes in cross section and more than 25 fields were measured in each group. All the images were measured using a quantitative digital image analysis system (Image-Pro Plus 6.0, Media Cybernetics, Rockville, MD).

Neonatal Rat Cardiomyocyte Culture and Infection With Recombinant Adenoviral Vectors

Neonatal rat cardiomyocytes (NRCMs) were prepared following methods that were previously described.[24] In short, 1- to 2-day-old Sprague-Dawley rats were sacrificed via swift decapitation according to the Guide for the Care and Use of Laboratory Animals published by the US National Institutes of Health. Then, the hearts were excised and extracted. Subsequently, the hearts were minced and digested with PBS containing 0.03% trypsin and 0.04% collagenase type II. The NRCMs were then seeded at a density of 1×10^6 cells/well in

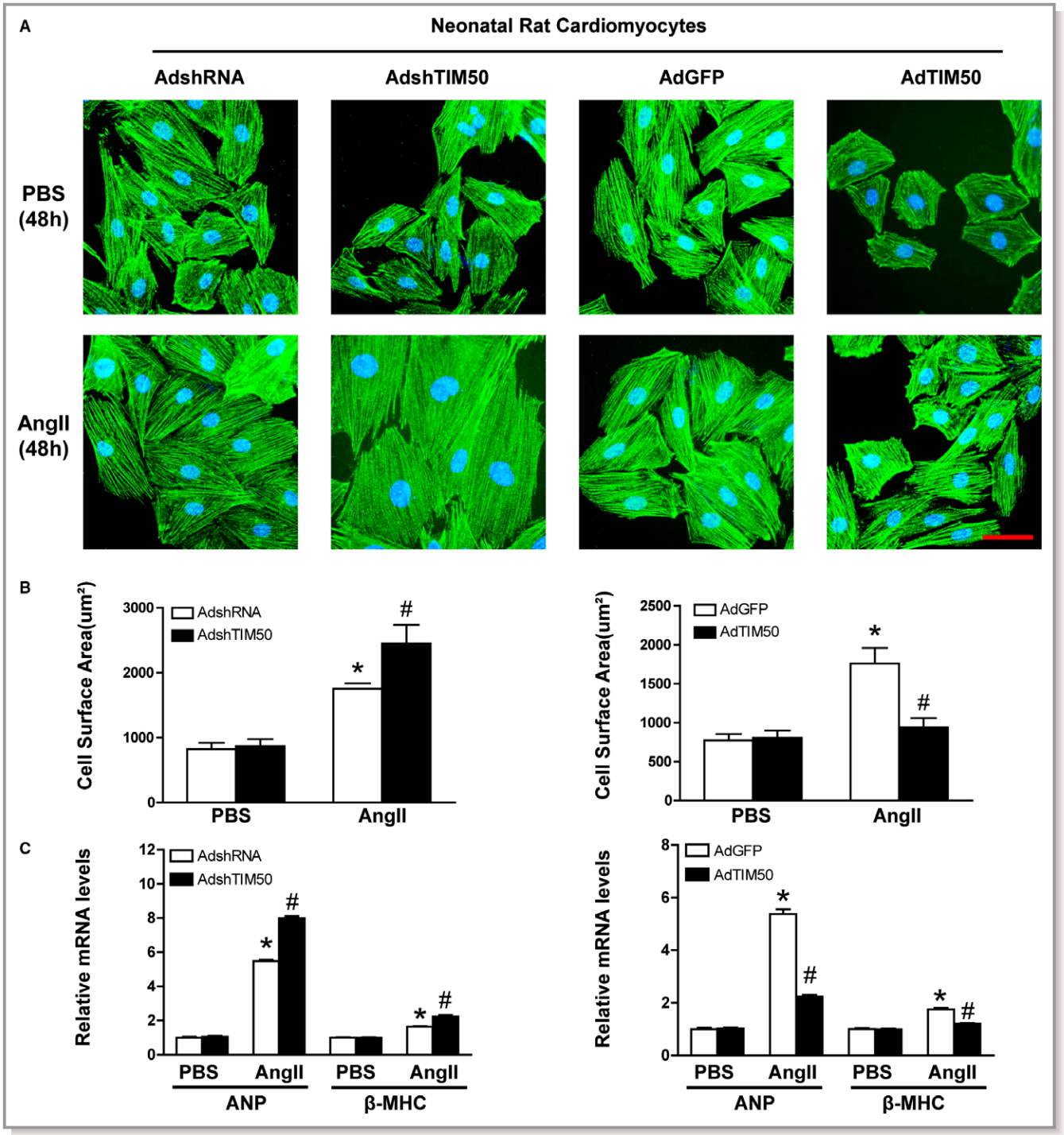

Figure 2. TIM50 attenuates cardiomyocyte hypertrophy in vitro. A, Representative immunofluorescence images of cardiomyocytes in the indicated group (green, α-actinin; blue, nuclei; scale bar, 20 μm). B, Calculated cell surface area in the indicated group (n>50 cells for each experimental group). C, Relative mRNA levels of prohypertrophic markers (n=3 independent experiments). **P*<0.05 vs AdshRNA/PBS or AdGFP/PBS group; #*P*<0.05 vs AdshRNA/Ang II or AdGFP/Ang II group; all data are presented as mean±SD. AdGFP indicates adenoviral vectors containing the green fluorescent protein gene; AdshRNA, adenoviral vectors containing the scramble shRNA sequence; AdshTIM50, adenoviral vectors containing the TIM50 shRNA sequence; AdTIM50, adenoviral vectors containing the TIM50 cDNA; PBS, phosphate-buffered saline; TIM50, translocase of inner membrane 50.

6-well culture plates coated with gelatin. The nutrient medium consisted of DMEM/F12 medium supplemented with 20% fetal calf serum, BrdU (0.1 mmol/L, to inhibit the proliferation of cardiac fibroblasts), and penicillin/streptomycin. After 48 hours the culture medium was replaced with serum-free DMEM/F12 for 12 hours to synchronize NRCMs. Then,

Table 2. Parameters in TIM50 KO and WT Mice at 4 Weeks After Sham Operation or AB

Parameters	Sham		AB	
	WT (n=12)	TIM50 KO (n=12)	WT (n=12)	TIM50 KO (n=12)
BW, g	25.20±1.16	26.07±1.14	26.57±1.84	26.98±2.55
HW/BW, mg/g	4.12±0.45	4.21±0.28	6.24±0.66*	8.31±0.86*†
LW/BW, mg/g	4.89±0.35	4.99±0.48	6.81±0.82*	10.47±2.03*†
HW/TL, mg/mm	5.89±0.67	6.11±0.66	9.18±0.44*	12.26±0.79*†
HR, beats/min	557.86±31.26	557.0±22.45	528.71±17.57	500.00±67.43
IVSd, mm	0.68±0.05	0.67±0.03	0.76±0.05*	0.81±0.05*†
LVDd, mm	3.37±0.27	3.16±0.10	4.19±0.26*	5.23±0.27*†
LVPWd, mm	0.64±0.05	0.64±0.05	0.76±0.05*	0.84±0.04*†
IVSs, mm	1.00±0.05	1.02±0.06	1.19±0.07*	1.25±0.05*†
LVDs, mm	1.87±0.24	1.80±0.12	2.87±0.27*	4.15±0.31*†
LVPWs, mm	1.04±0.08	1.02±0.06	1.23±0.10*	1.28±0.08*
EF, %	82.86±2.19	79.57±3.55	59.71±7.85*	43.33±2.58*†
FS, %	44.43±3.10	43.00±2.24	31.71±2.43*	20.83±2.04*†

All values are presented as mean±SD. AB indicates aortic banding; BW, body weight; EF, ejection fraction; FS, fractional shortening; HR, heart rate; HW, heart weight; IVS, interventricular septal thickness; LVD, left ventricular dimension; LVPW, left ventricular posterior wall; LW, lung weight; TL, tibia length.
*P<0.05 vs WT sham operation.
†P<0.05 vs WTAB 4 weeks after AB.

NRCMs were treated with PBS and angiotensin II (Ang II, 0.1 μmol/L) for 48 hours to induce cardiomyocyte hypertrophy.

To overexpress TIM50, the rat TIM50 gene under the control of the cytomegalovirus promoter was inserted into replication-defective adenoviral vectors. A similar adenoviral vector encoding the green fluorescent protein (GFP) gene was used as a control. To reduce TIM50 expression, 3 rat shTIM50 constructs were obtained from SABiosciences (KR45645G, Valencia, CA); among the 3 constructs, the 1 that inhibited TIM50 expression to the greatest extent was selected for the subsequent experiments. AdshRNA was used as a control for AdshTIM50. NRCMs were infected with AdGFP, AdTIM50, AdshRNA, and AdshTIM50 in diluted media at a multiplicity of infection of 100 for 24 hours.

Immunofluorescence

After the NRCMs were infected with adenovirus and treated with PBS or Ang II (0.1 μmol/L) for 48 hours, the cardiomyocytes were fixed with 100% methanol for 20 minutes at room temperature to quench the GFP signal, and NRCMs were then permeabilized with 0.1% Triton X-100 in PBS for 40 minutes and stained with α-actinin (1:100 dilution) following standard immunofluorescence staining procedures. The NRCMs were visualized using a fluorescence microscope (Olympus, Tokyo, Japan) and measured with a quantitative digital image analysis system (Image-Pro Plus 6.0, Media Cybernetics, Rockville, MD). More than 50 cells were visualized in each experimental group.

Quantitative Real-Time PCR

Total mRNA was extracted from mouse ventricular tissue and NRCMs using TRIzol (Invitrogen, Carlsbad, CA). cDNA was cloned from oligo-dT primers using reverse transcription PCR (RT-PCR) with a Transcriptor First Strand cDNA Synthesis Kit (Roche Molecular Diagnostics, Pleasanton, CA). Selected gene expression was measured through quantitative real-time PCR using SYBR Green (Roche); the results were normalized as the ratio of target gene/GAPDH gene expression. The primers used in the present study are listed in Table 1.

Western Blotting

Total proteins were extracted from ventricular tissue and NRCMs in lysis buffer (720 μL RIPA, 20 μL PMSF, 100 μL Complete, 100 μL Phos-stop, 50 μL NaF, 10 μL Na_3VO_4 in 1 mL lysis buffer), and the protein concentrations were measured using a Pierce® BCA Protein Assay Kit (Pierce, Rockford, IL). Then, 20 μg of protein for each sample was separated using SDS-PAGE (Invitrogen, Carlsbad, CA) and electrically transferred to polyvinylidene fluoride membranes (Millipore, Billerica, MA). The polyvinylidene fluoride membranes were subsequently blocked in tris-buffered saline with

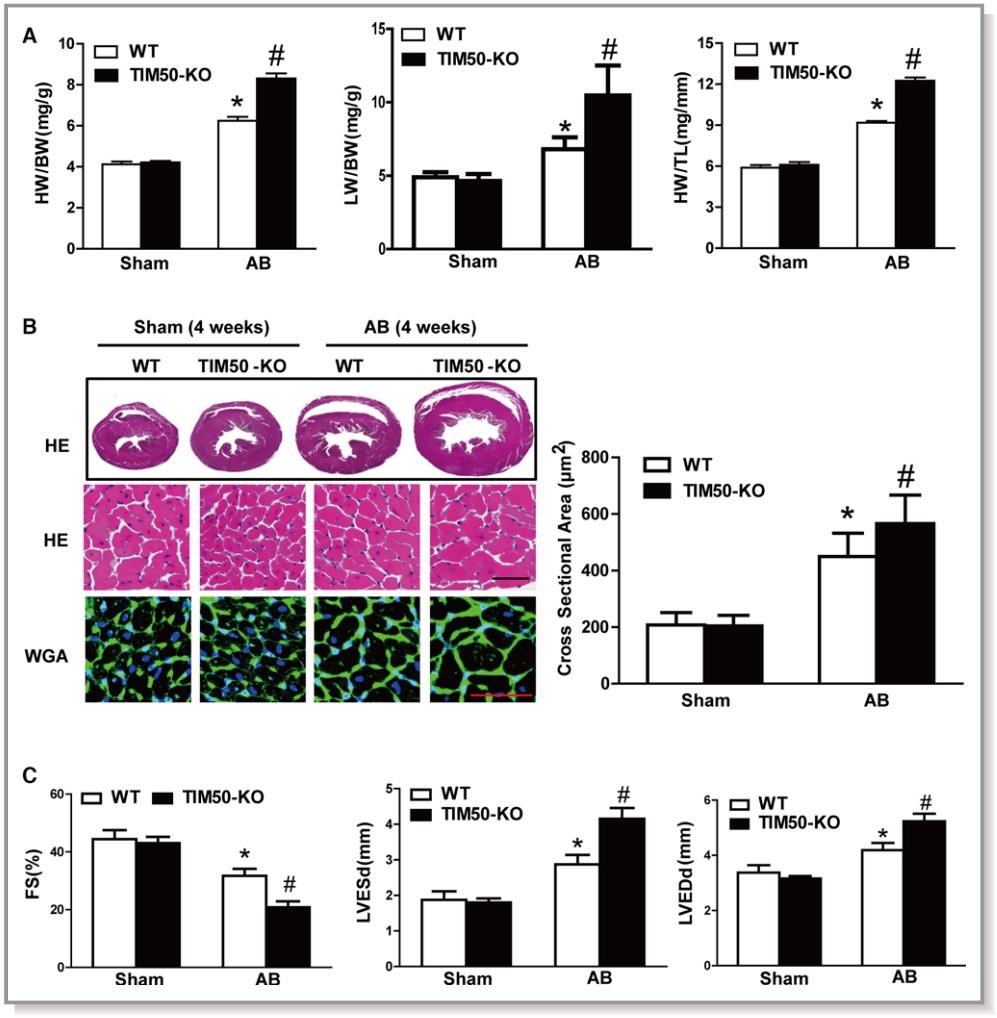

Figure 3. TIM50 deficiency exacerbates pathological cardiac hypertrophy. A, Ratios of heart weight (HW) to body weight (BW), lung weight (LW) to BW and HW to tibia length (TL) in the indicated group (n=10-12 mice for each experimental group). B, Left: Hematoxylin and eosin (HE) and wheat germ agglutinin (WGA) staining of heart samples in the indicated group. B, Right: Calculated cross-sectional area of heart samples (n>100 cells for each group, scale bar middle and bottom 50 μm). C, Parameters of echocardiography analysis in the indicated group (n=5-6 for each experimental group). D, Left: Cardiac fibrosis in perivascular and interstitial area of the heart samples (n>25 fields for each group). D, Right: Calculated left ventricular collagen volume (LVCV) in the indicated group. E, Relative mRNA level of collagen Iα, collagen III, and connective tissue growth factor (CTGF) in the indicated group (n=4 for each experimental group). *P<0.05 vs Sham group; $^{\#}P$<0.05 vs WT/AB group. All data are presented as mean±SD. TIM50 indicates translocase of inner membrane 50.

Tween 20 containing 5% skimmed milk powder for 90 minutes at room temperature and incubated with different primary antibodies overnight at 4°C. The next day the membranes were incubated with secondary peroxidase-conjugated antibody (Jackson ImmunoResearch Laboratories, West Grove, PA) at a 1:10 000 dilution, and signals were visualized with FluorChem E (Cell Biosciences, Santa Clara, CA). Protein expression was normalized as the ratio of target protein/GAPDH that had been transferred to the same polyvinylidene fluoride membrane.

Measurement of Enzyme Activity

Measurement of SOD Activity

The method has been previously described.[25] Briefly, the heart homogenate was incubated with 0.1 mol/L PBS and then centrifuged at 100 000g for 1 hour at 4°C. The supernatant was dialyzed overnight and then preincubated with a reaction mixture (0.043 mol/L Na_2CO_3 buffer [pH 10.2], 0.1 mmol/L xanthine, 0.1 mmol/L EDTA, 0.05 mg/mL bovine serum albumin, 0.025 mmol/L nitro blue tetrazolium)

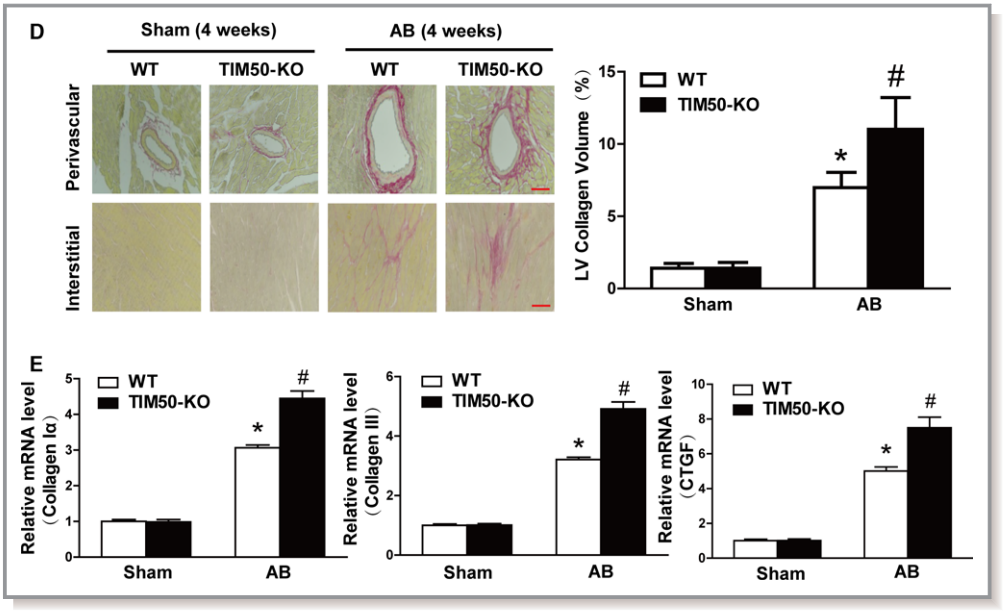

Figure 3. Continued

for 10 minutes at 25°C. The reaction was started by adding 0.1 mL xanthine oxidase for 20 minutes at 25°C. The absorbance at 560 nm was measured after the addition of 0.2 mmol/L $CuCl_2$.

Measurement of Catalase Activity

The method used to measure catalase activity was previously described.[11] In brief, heart homogenate was incubated with 0.1 mol/L PBS and then centrifuged at 100 000*g* for 1 hour at 4°C. The heart homogenate was then incubated in 0.1 mol/L PBS with 0.45 mol/L H_2O_2. The mixture was then removed at 20-second intervals and transferred to 2.0 mL of mixture (0.2 mg/mL O-dianisidine, 0.015 mg/mL peroxidase, and 0.81 mg/mL sodium azide). Then, 50% H_2SO_4 solution was added to stop the reaction after incubation for 10 minutes at room temperature. The absorbance of the reaction mixture was measured at 530 nm.

Measure of OXPHOS activity

The activities of complexes I (MS141), II (MS241), and IV (MS444) were measured using kits purchased from MitoSciences Corporation (Eugene, OR). Sample preparation and experimental methods were strictly performed following the manufacturer's instructions. The detailed procedure has been described previously.[11] Briefly, complex I activity was determined by following the oxidation of NADH to NAD^+ and the simultaneous reduction of a dye, which leads to increased absorbance at OD=450 nm. Complex II activity was determined by following a decrease in the absorbance at 600 nm because the production of ubiquinol by the enzyme is coupled to reduction of the dye 2,6-diclorophenolindophenol (DCPIP). Complex IV activity (cytochrome c oxidase activity) was determined colorimetrically by following the oxidation of reduced cytochrome c by the absorbance change at 550 nm.

Statistical Analysis

The data are presented as the mean±SD. Differences among groups were assessed using 1-way analysis of variance (ANOVA) and then a Bonferroni test (assuming equal variances) or Tamhane T2 test (without the assumption of equal variances). Comparisons between 2 groups were performed using Student t test. A value of $P<0.05$ was considered to indicate a statistically significant difference.

Results

TIM50 Expression Is Decreased in Human DCM Hearts and Hypertrophic Murine Hearts

To explore the potential role of TIM50 in cardiac hypertrophy and heart failure, we first examined whether the expression of TIM50 was altered in human DCM hearts. Western blot results indicated that the protein level of TIM50 was apparently decreased in all DCM hearts compared with donor hearts. Moreover, the cardiac hypertrophic markers atrial natriuretic peptide (ANP) and β-myosin heavy chain (β-MHC) were both markedly elevated with the downregulation of TIM50 (Figure 1A). Consistent with the results in human DCM hearts, the cardiac hypertrophic murine model induced

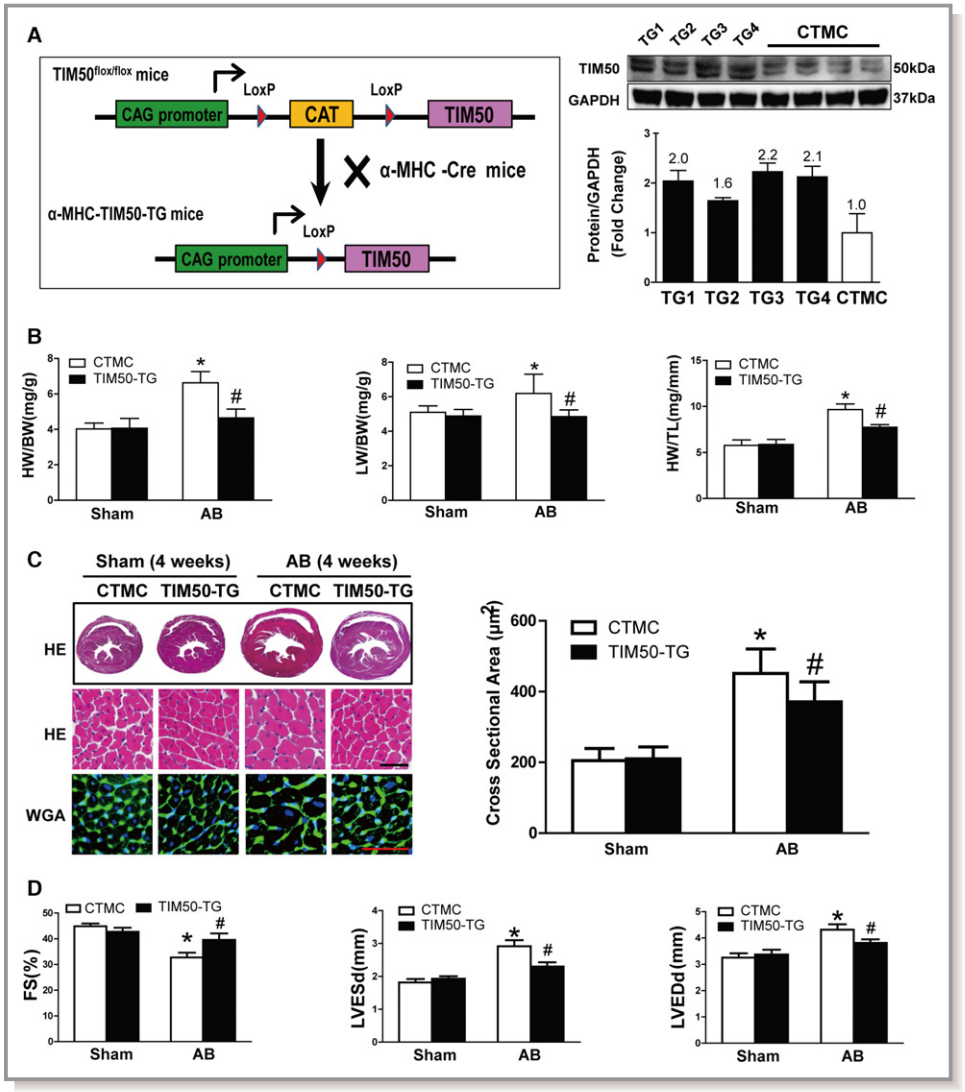

Figure 4. TIM50 overexpression in cardiomyocytes protects against pathological cardiac hypertrophy. A, Left: Schematic diagram of cardiac-specific TIM50 transgenic mice. A, Right: Expression of TIM50 in CAG-CAT-TIM50/MHC-Cre mice without tamoxifen administration (CTMC) and TIM50-transgenic (TG) mice (n=4 for each experimental group). B, HW/BW, LW/BW, and HW/TL in the indicated group (n=12 mice per experimental group). C, Left: Histological analysis of HE and WGA staining in the indicated group (n=5-6 mice per experimental group. Scale bars, middle and bottom, 50 μm). C, Right: Statistical results for the cross-sectional area in the indicated groups (n>100 cells for each experimental group). D, Echocardiography results for CTMC and TIM50-TG mice in the indicated group (n=6-8 for each experimental group). E, Left: Cardiac fibrosis in perivascular and interstitial area of the heart samples (n>25 fields for each group). E, Right: Calculated LVCV in the indicated group (n>25+ fields for each experimental group). F, The relative mRNA levels of the fibrotic markers collagen Iα, collagen III, and CTGF in the indicated group (n=4 for each experimental group). *P<0.05 vs CTMC/sham; $^{\#}P$<0.05 vs CTMC/AB. All of the data are presented as the mean±SD. AB indicates aortic band; BW, body weight; CAG, chicken beta-actin; CAT, chloramphenicol acetyltransferase; CTMC, CAG-CAT-mTIM50/MHC-Cre mice without tamoxifen injection; CTGF, connective tissue growth factor; HE, hematoxylin-eosin; HW, heart weight; LVCV, left ventricular collagen volume; LW, lung weight; TIM50, translocase of inner membrane 50; TL, tibia length; WGA, wheat germ agglutinin.

by AB showed a remarkable decline of TIM50 expression compared with sham-operated mice, and ANP and β-MHC were increased after AB treatment (Figure 1B). Meanwhile, the hypertrophic cardiomyocytes treated with Ang II for 24 and 48 hours also demonstrated a significant decrease of TIM50 (Figure 1C). Taken together, these results enhanced

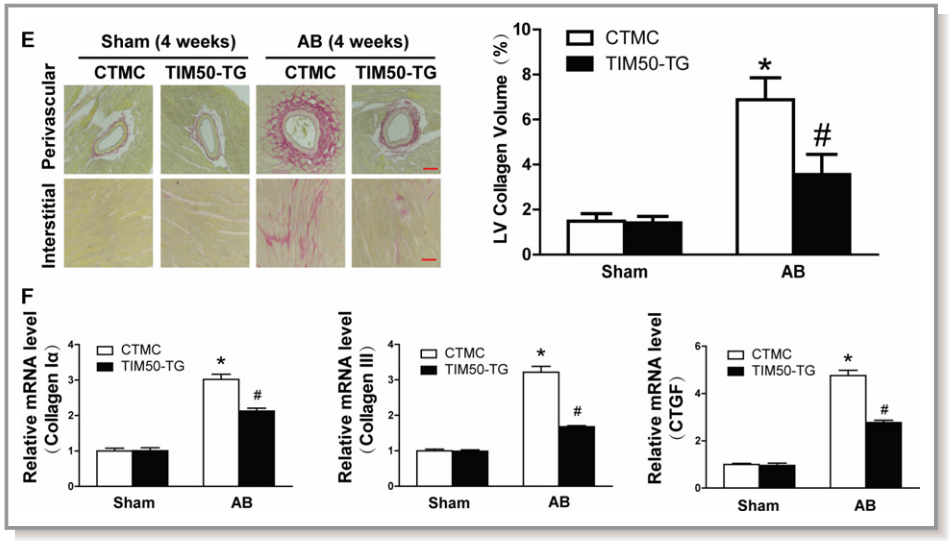

Figure 4. Continued.

the possible relationship between TIM50 and pathological cardiac hypertrophy.

TIM50 Attenuates Cardiomyocyte Hypertrophy Induced by Ang II In Vitro

Because TIM50 expression was obviously altered in human DCM hearts, cardiac hypertrophic murine hearts, and cardiomyocytes, we decided to explore the contribution of TIM50 to cardiac hypertrophy. First, cultured NRCMs were infected with AdshTIM50, AdTIM50, or control vectors (Figure S1). Then, NRCMs were stimulated using Ang II for 48 hours to induce cardiomyocyte hypertrophy. Under basal conditions (PBS treatment), no differences in cell size and morphology were observed after adenovirus injection. However, immunostaining with an α-actinin antibody indicated that AdshTIM50 treatment increased the cell area, whereas the overexpression of TIM50 (AdTIM50) decreased the cell size exposed to Ang II compared with controls (Figure 2A and 2B). Accordingly, the mRNA levels of hypertrophic markers (ANP, β-MHC) were significantly higher in the AdshTIM50-infected cardiomyocytes and dramatically decreased in the AdTIM50-infected cells (Figure 2C). In general, our results indicated that TIM50 attenuated Ang II-induced cardiac hypertrophy in vitro.

TIM50 Deficiency Deteriorates Cardiac Hypertrophy Induced by Pressure Overload In Vivo

To illustrate the role and effects of TIM50 in cardiac hypertrophy in vivo, a mouse model with a global knockout of TIM50 (TIM50 KO) was generated, in which TIM50 expression in the heart was completely deficient (Figure S2A through S2E). At baseline, TIM50 KO mice displayed few pathological structural and functional alterations in the heart (Table 2). However, 4 weeks after AB, TIM50 KO mice showed significantly enhanced cardiac hypertrophy compared with their wild-type (WT) littermates, as indicated by the increased heart weight (HW)/body weight (BW), lung weight (LW)/BW and HW/tibial length (TL) ratios (Figure 3A). Histological examination revealed increased cross-sectional area of cardiomyocytes in TIM50 KO mice compared with WT mice 4 weeks after AB (Figure 3B). Moreover, echocardiographic analysis demonstrated increased left ventricular chamber dimension with impaired systolic function (Figure 3C). To further elucidate the function of TIM50 in maladaptive cardiac hypertrophy, paraffin-embedded slides were stained with picrosirius red to determine cardiac fibrosis, a hallmark of pathological cardiac hypertrophy. Both interstitial and perivascular fibrosis were significantly increased in AB-treated WT hearts and tended to be more severe in TIM50 KO hearts (Figure 3D). Expression of the fibrotic markers collagen Iα, collagen III, and connective tissue growth factor was dramatically elevated in TIM50 KO mice compared with WT mice in response to pressure overload (Figure 3E). Collectively, these loss-of-function data elucidated that TIM50 deficiency deteriorated the pathological cardiac remodeling induced by chronic pressure overload.

TIM50 Overexpression Inhibits Pressure Overload–Induced Cardiac Hypertrophy In Vivo

To further determine whether TIM50 overexpression in the heart has a protective role in cardiac hypertrophy, we generated cardiac-specific TIM50 transgenic mice (TG mice) (Figure 4A). The TG mice exhibited normal cardiac structure and function after birth (Table 3), but 4 weeks after AB

surgery, the HW/BW, LW/BW, and HW/TL ratios were all profoundly decreased in TG mice compared with CTMC mice (Figure 4B). HE and WGA staining results showed similar results (Figure 4C). Consistent with these results, cardiac function was pronouncedly improved in TG mice compared with CTMC mice (Figure 4D). Cardiac fibrosis in both interstitial and perivascular areas was also mitigated in TG mice, along with decreased mRNA levels of fibrosis markers (collagen Iα, collagen III, and connective tissue growth factor) (Figure 4E and 4F). Together, these results indicated that TIM50 overexpression alleviated cardiac hypertrophy after AB operation.

TIM50 Regulates Oxidative Stress, Apoptosis, and Related Signaling Pathways

Various studies have indicated that mitochondrial proteins impact cardiac hypertrophy via regulating oxidative stress.[11,26] Thus, we examined the ROS generation and the activity of 2 key antioxidant enzymes in both TIM50 gain- and loss-of-function mice. As expected, ROS generation was significantly increased in TIM50 KO mice and decreased in TIM50-TG mice compared with their respective controls (Figure 5A). Because TIM50 regulates apoptosis and ROS can induce cell apoptosis, we next performed dihydroethidium staining and detected the cleaved-caspase-3 expression level to measure apoptosis status for each group. In accordance with ROS generation level, apoptosis level was elevated in TIM50 KO mice and decreased in TIM50-TG mice (Figure 5B). Furthermore, the activities of SOD and catalase were both reduced in TIM50 KO mice 4 weeks after AB, whereas the transgenic mice showed elevated enzyme activity (Figure 5C), which indicated that TIM50 could activate antioxidative enzymes to eliminate oxidative stress. Respiratory chain complexes are major sites for ROS generation, and defects in these complexes aggravate oxidative stress. Hence, we next examined the activities of complexes I, II, and IV. As shown in Figure 5D and 5E, the activities of all 3 complexes were significantly decreased in TIM50 KO mice, whereas TIM50 transgenic mice showed enhanced activities. TIM50 is an important receptor for mitochondrial protein translocation, so we measured the mitochondrial morphology and biogenesis-related protein level to figure out whether TIM50 influences mitochondrial dynamics. As seen in Figure S3, there was no difference in Drp-1, Mfn1, Mfn2, or Nrf2 expression in each group, which implies that TIM50 may not affect mitochondrial dynamics. These data indicated that TIM50 may regulate both antioxidant enzyme and respiratory complex activity to reduce oxidative stress.

Excessive oxidative stress can activate MAP-kinase (MAPK) signaling during pathological cardiac hypertrophy.[27] Thus, we[27] assessed whether TIM50 has an effect on MAPK signaling. As shown in Figure 6A through 6D, phosphorylated JNK and P38 levels were dramatically increased in TIM50-deficient mice and cardiomyocytes, whereas in TIM50 transgenic mice, p-JNK and p-P38 levels were relatively lower compared with those of the control group. However, the

Table 3. Parameters in CTMC Mice and TIM50 Transgenic Mice at 4 Weeks After Sham Operation or AB

	Sham		AB	
Parameters	CTMC (n=12)	TIM50 TG (n=12)	CTMC (n=12)	TIM50 TG (n=12)
BW, g	25.36±1.95	25.56±1.50	25.57±1.98	26.51±3.38
HW/BW, mg/g	4.02±0.33	4.06±0.55	6.63±0.64*	4.64±0.83*†
LW/BW, mg/g	5.10±0.37	4.88±0.38	6.80±2.36*	4.85±0.39†
HW/TL, mg/mm	5.77±0.60	5.87±0.55	9.65±0.62*	7.74±0.27*†
HR, beats/min	534.71±26.54	563.0±22.45	523.57±19.24	540.71±31.88
IVSd, mm	0.67±0.03	0.68±0.02	0.73±0.04*	0.69±0.02†
LVDd, mm	3.26±0.16	3.37±0.18	4.31±0.20*	3.81±0.03*†
LVPWd, mm	0.68±0.02	0.68±0.05	0.76±0.02*	0.69±0.03†
IVSs, mm	1.00±0.02	0.99±0.03	1.17±0.05*	1.06±0.08†
LVDs, mm	1.81±0.11	1.93±0.08	2.91±0.19*	2.30±0.13*†
LVPWs, mm	1.00±0.02	1.03±0.05	1.19±0.04*	1.11±0.07*†
EF, %	82.00±1.53	81.00±1.29	68.14±4.98*	77.71±3.64*†
FS, %	44.50±0.05	43.00±1.55	32.71±1.89*	39.57±2.51*†

All values are presented as mean±SD. AB indicates aortic banding; BW, body weight; CTMC, CAG-CAT-mTIM50/MHC-Cre mice without tamoxifen injection; EF, ejection fraction; FS, fractional shortening; HR, heart rate; HW, heart weight; IVS, interventricular septal thickness; LVD, left ventricular dimension; LVPW, left ventricular posterior wall; LW, lung weight; TL, tibia length.
*P<0.05 vs CTMC sham operation.
†P<0.05 vs CTMC AB after 4 weeks AB.

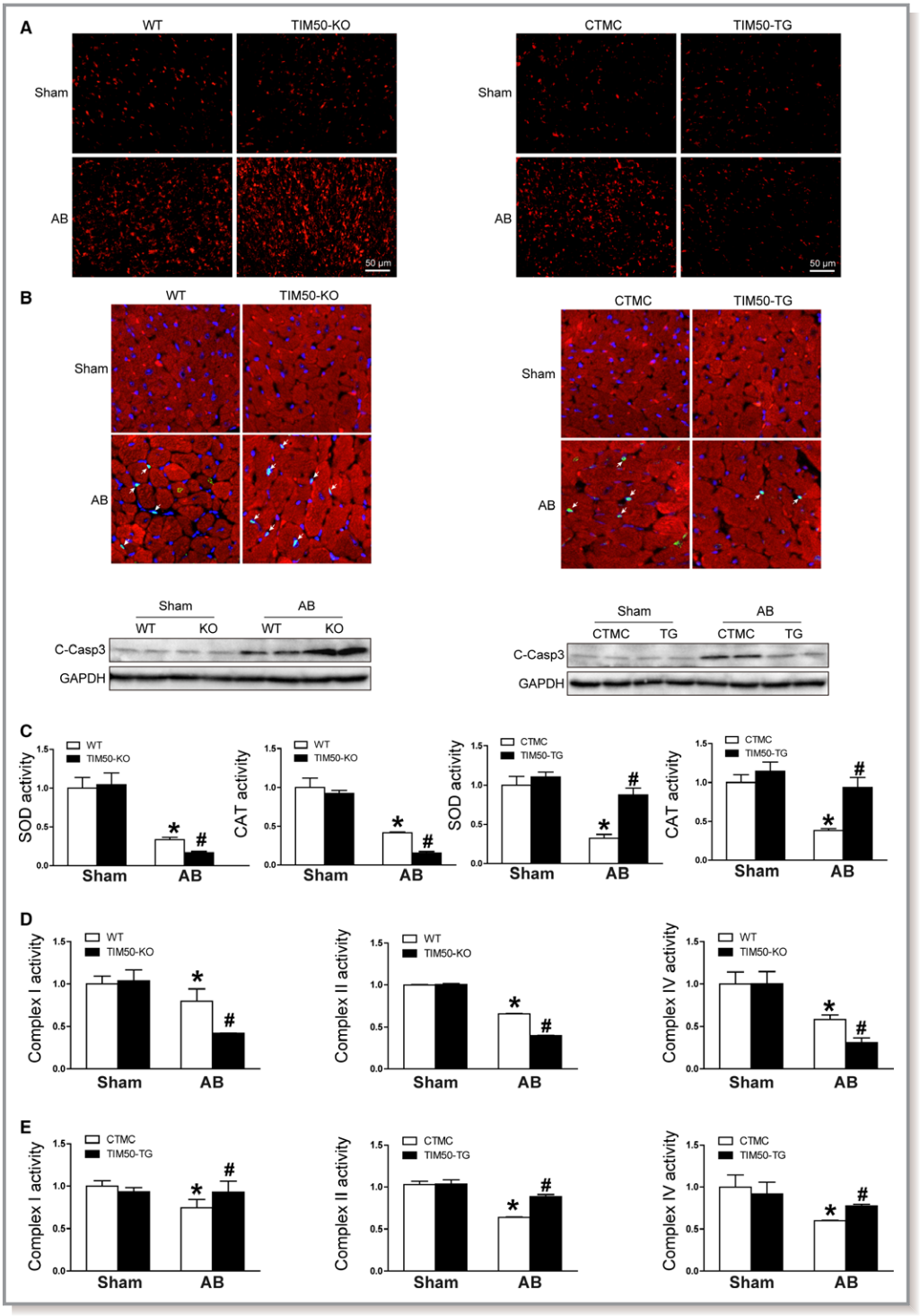

Figure 5. TIM50 regulates ROS generation, apoptosis, antioxidant enzymes, and respiratory chain complex activity under hypertrophic stimuli. A, DHE staining to display ROS generation in heart samples in the indicated group. B, Upper: DHE staining to indicate apoptosis level in the indicated group. B, Bottom: expression level of cleaved-caspase 3 in the indicated group. C, Fold change of SOD and catalase activity in the indicated group (n=6 for each experimental group). D, Fold change of respiratory chain complexes I, II, and IV in wild-type (WT) and TIM50 KO mice after sham or AB operation (n=6 for each experimental group). E, Fold change of respiratory chain complexes I, II, and IV in CTMC and TIM50 TG mice after sham or AB operation (n=6 for each experimental group). AB indicates aortic banding; CTMC, CAG-CAT-mTIM50/MHC-Cre mice without tamoxifen injection; DHE, dihydroethidium; KO, knockout; ROS, reactive oxygen species; SOD, superoxide dismutase; TG, transgenic; TIM50, translocase of inner membrane 50. **P*<0.05 vs CTMC/sham, $^{\#}$*P*<0.05 vs CTMC/AB.

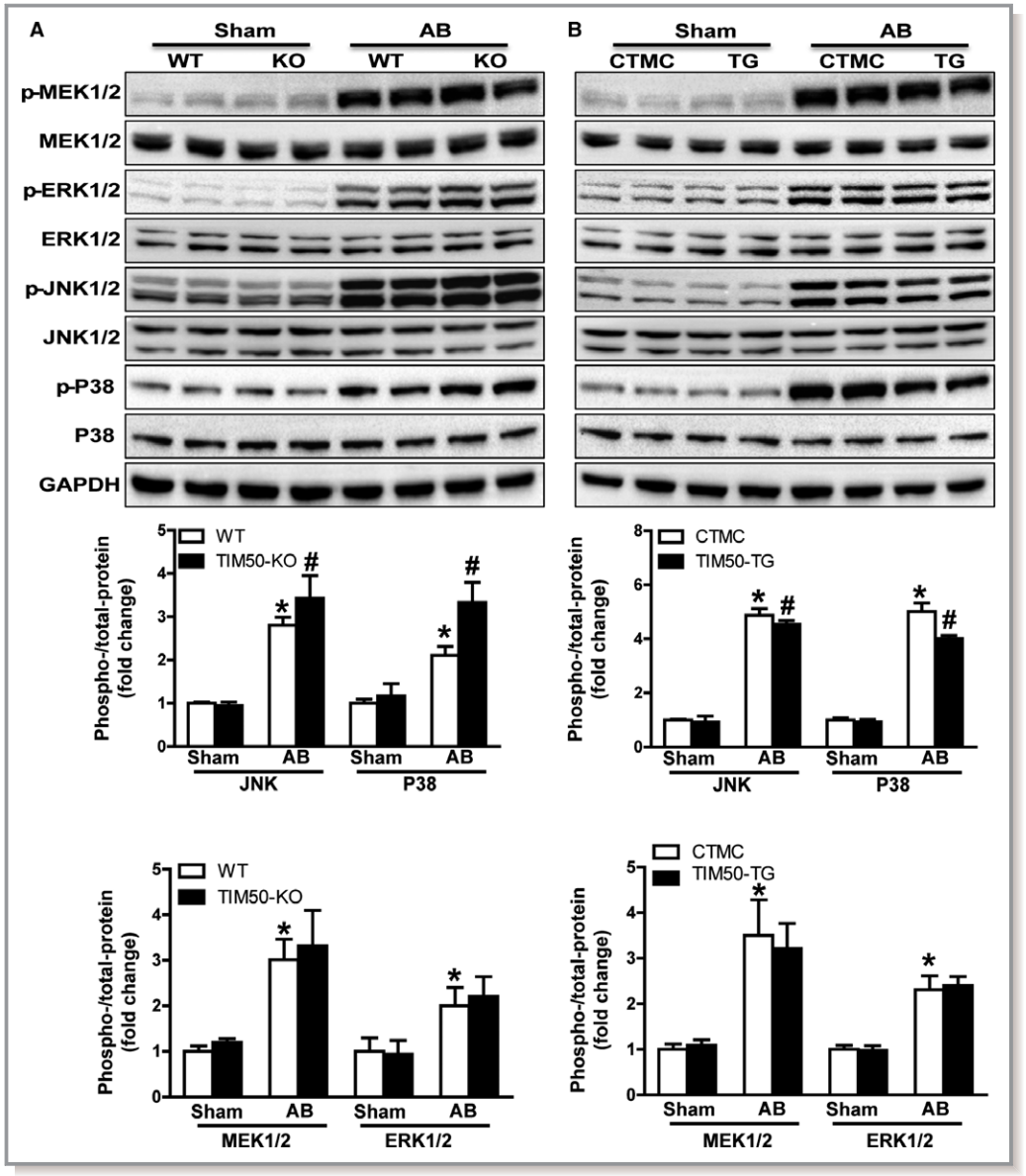

Figure 6. TIM50 regulates the ASK1-JNK/P38 axis in hypertrophic hearts. A and B, Western blot analysis of MAPK signaling components in WT and TIM50 KO mice (A) or CTMC and TIM50 TG mice (B) (n=6 for each experimental group). C and D, Western blot analysis of MAPK signaling components in AdshRNA and AdshTIM50 cardiomyocytes (C) or AdGFP and AdTIM50 cardiomyocytes (D) (n=3 independent experiments). E and F, expression of ASK1 and phospho-ASK1 in WT and TIM50 KO mice (E) or CTMC and TIM50 TG mice (F) (n=6 for each experimental group). G and H, expression of ASK1 and phospho-ASK1 in AdshRNA and AdshTIM50 cardiomyocytes (G) or AdGFP and AdTIM50 cardiomyocytes (H) (n=3 independent experiments). **P*<0.05 vs WT/sham, CTMC/sham, AdshRNA/PBS, or AdGFP/PBS group; $^{\#}P$<0.05 vs WT/AB, CTMC/AB, AdshRNA/Ang II or AdGFP/Ang II group. All data are presented as mean±SD. Ad indicates adenoviral vectors; AdshRNA, adenoviral vectors containing the scramble shRNA sequence; Ang II, Angiotensin II; CTMC, CAG-CAT-mTIM50/MHC-Cre mice without tamoxifen injection; GFP, green fluorescent protein; KO, Knockout; MAPK, mitogen-activated protein kinase; PBS, phosphate-buffered saline; TG, Transgenic; TIM50, translocase of inner membrane; 50 WT, wild type.

MEK1/2 and ERK1/2 activities were not significantly changed in either TIM50 deficiency or overexpression group after hypertrophic stress. Furthermore, because ASK1 is activated by oxidative stress and also acts as an upstream regulator of both JNK and P38, we examined ASK1 expression. Not surprisingly, phosphorylated ASK1 was upregulated in the TIM50 deficiency group and downregulated in the TIM50 overexpression group after hypertrophic stimuli (Figure 6E through 6H). Altogether, these results indicated that TIM50 attenuates oxidative stress, further

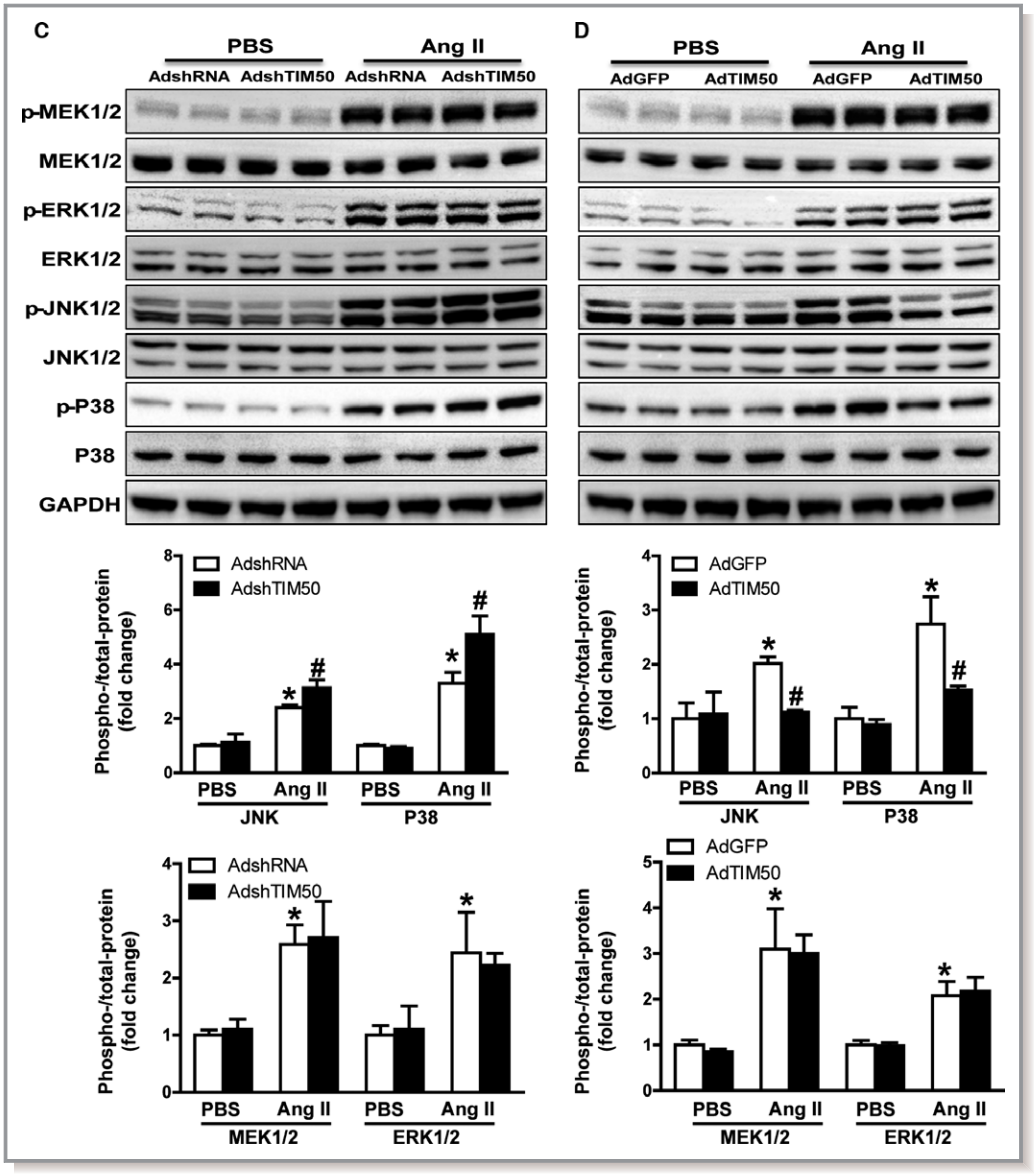

Figure 6. Continued

inhibiting the activity of ASK1 during pathological cardiac hypertrophy.

The Inhibition of Oxidative Stress Dramatically Reduced Cardiac Hypertrophy in TIM50 KO Mice

To further consolidate our results, the mice were pretreated with NAC, an antioxidant that is universally used to reduce oxidative stress. After NAC administration, phosphorylated ASK1, JNK, and P38 levels were decreased (Figure 7A). Meanwhile, the HW/BW, LW/BW, and HW/TL ratios were also decreased to a similar level, along with a reduced cross-sectional area between wild-type and TIM50 KO mice (Figure 7B and 7C). Cardiac function was also significantly improved after NAC treatment, as indicated by increased fractional shortening accompanied with decreased LV end-diastolic diameter and LV end-systolic diameter (Figure 7D). Cardiac fibrosis was also alleviated after NAC treatment (Figure 7E). These data further confirmed that TIM50 regulates cardiac hypertrophy primarily by reducing oxidative stress.

Discussion

Cardiac hypertrophy is a common pathological condition that ultimately leads to heart failure. The mitochondrial import pathway is of great importance for mitochondrial function because most proteins are transported into mitochondria from the cytosol. Moreover, mitochondria, as the energy factories of cells, comprise 30% of the cardiomyocyte volume.[28] However, the role of TIM50, as a critical component

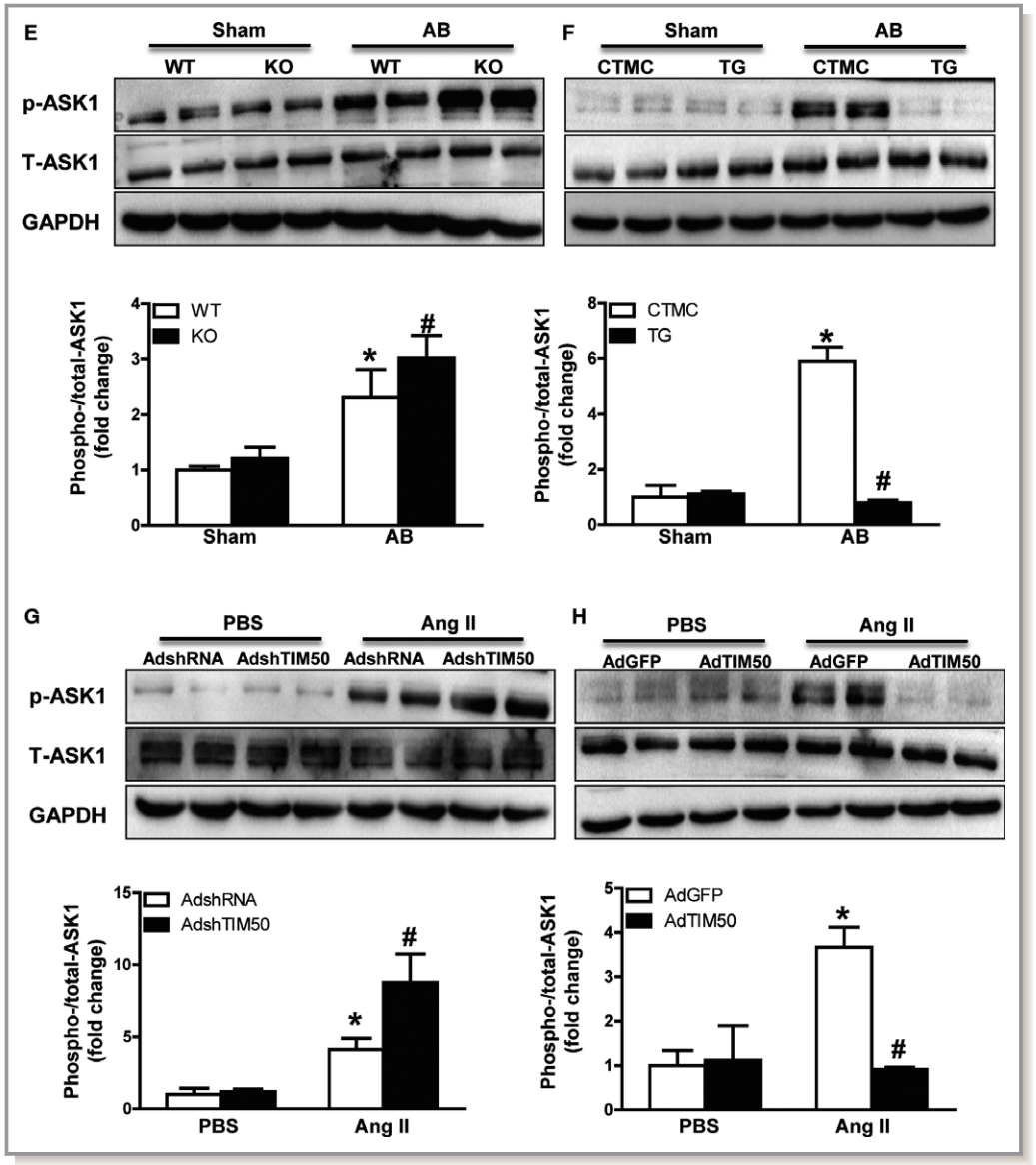

Figure 6. Continued

of the TIM23 complex, remains unclear in the heart. In the present study we utilized both TIM50 global KO mice and cardiac-specific transgenic mice to decipher the role of TIM50 in pressure-overload–induced cardiac hypertrophy. We demonstrated that TIM50 regulates cardiac hypertrophy and function primarily by reducing oxidative stress. To our knowledge this study is the first to show that TIM50 is a pivotal intrinsic negative regulator of cardiac hypertrophy.

Growing evidence highlights oxidative stress as an important mechanism for the maladaptation of cardiac hypertrophy.[29] The mitochondrial antioxidant system is the key factor that regulates the balance of oxidative stress, and so it is interesting to elucidate whether TIM50 can influence the enzyme activity during pathological cardiac hypertrophy. In the present study we discovered that ROS generation was regulated by TIM50. Moreover, the activities of some major antioxidant enzymes, such as SOD and catalase were enhanced by TIM50 overexpression, whereas the absence of TIM50 inhibited their activities. These findings are consistent with our and others' previous studies indicating that both SOD and catalase have protective effects during cardiac hypertrophy.[30,31] The possible mechanism by which TIM50 regulates the activities of these enzymes may be dependent on the binding of TIM50 with TIM23, resulting in closure of the TIM23 channel in the absence of substrates,[32] further preventing ion leakage and ROS generation (Figure 8). The inhibition of ROS accumulation could improve antioxidant system expression and activity in the mitochondria. Notably, the deficiency of another mitochondrial translocase complex, TOM70, aggravates pathological cardiac hypertrophy with increased ROS levels.[17] Because TOM70 and TIM50 both function as receptors of the complex, further research must elucidate

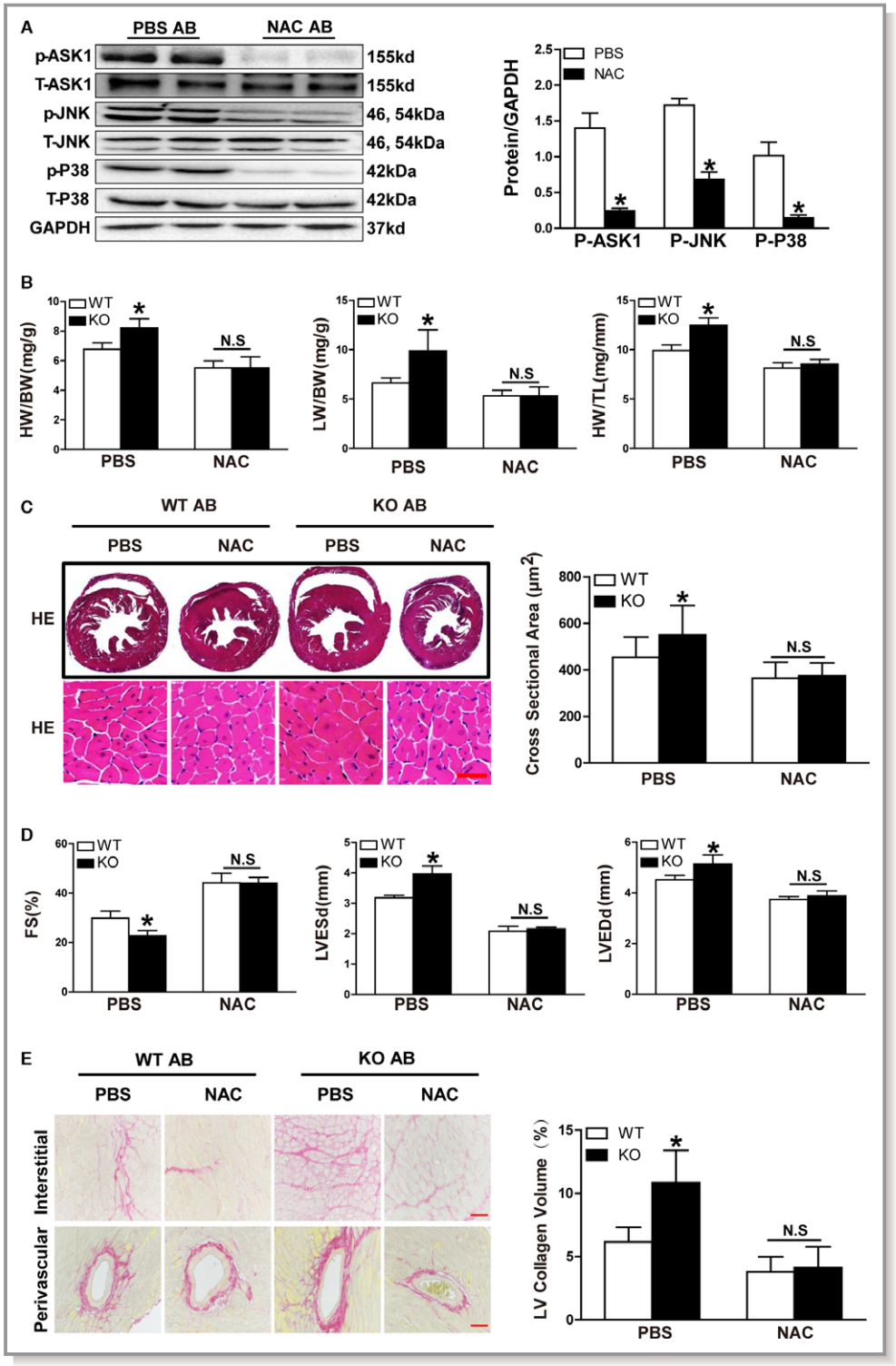

Figure 7. NAC treatment is sufficient to reverse pathological cardiac hypertrophy in TIM50 KO mice. A, Western blot analysis to indicate ASK1, JNK, and P38 expression in the indicated group (n=6 for each experimental group). B, HW/BW, LW/BW and HW/TL in the indicated group (n=8 for each experimental group). C, HE staining to indicate heart size and cardiomyocyte cross-sectional area in the indicated group (n=4-5 for each experimental group). D, Parameters of echocardiography in the indicated group (n=8 for each experimental group). E, PSR staining to indicate cardiac fibrosis in the indicated group (n=4-5 for each experimental group). *P<0.05 vs WT AB/PBS group; NS, not significant. All data are presented as mean±SD. AB indicates aortic banding; BW, body weight; HE, hematoxylin-eosin; KO, knockout; LW, lung weight; NAC, N-acetyl cysteine; PSR, picrosirius red; TIM50, translocase of inner membrane 50; TL, tibia length.

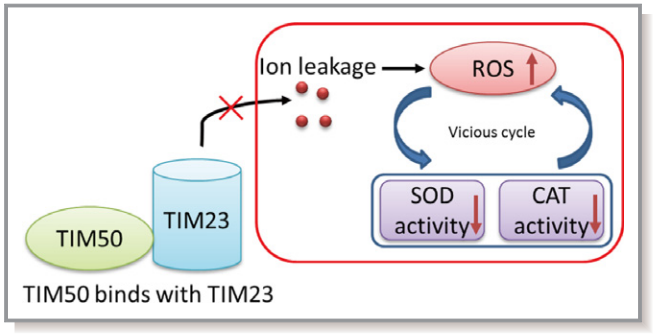

Figure 8. Schematic diagram of a possible mechanism of how TIM50 regulates ROS generation. TIM50 can directly bind with TIM23, which causes the closure of the ion channel to prevent the ion leakage. Ion leakage reduction further decreases the ROS generation. Excessive ROS generation impairs the SOD and catalase activities, which in turn increase the ROS generation, forming a vicious cycle. CAT indicates catalase; ROS, reactive oxygen species; SOD, superoxide dismutase; TIM50 and TIM23, translocases of the inner membrane.

whether TIM50 could directly regulate ROS generation during cardiac hypertrophy.

In addition to the antioxidant system, the mitochondrial respiratory chain also regulates oxidative stress.[5] Ion leakage from the respiratory complex is a major source of ROS generation. Previous studies illustrate that mitochondrial OXPHOS dysfunction is associated with increased ROS levels. Moreover, mitochondrial OXPHOS deficiencies have been documented in heart failure and hypertrophic cardiomyopathy.[33] Because a vast majority of respiratory chain subunits and assembly factors are imported with the help of the TIM23 complex,[34] it is possible that the alteration of TIM50 expression may influence the activity of OXPHOS. Here, in accordance with our hypothesis, the activities of respiratory complexes I, II, and IV were decreased in TIM50 KO mice and increased in TIM50 TG mice under hypertrophic stress. Our data indicated that TIM50 could improve the activities of the antioxidant system and OXPHOS system, which are 2 vital systems related to oxidative stress. However, the precise regulatory mechanism must to be studied further. Another interesting finding in the present study was that TIM50 did not regulate mitochondrial morphology and biogenesis (Figure S3). In our perspective, some other mitochondrial translocases, such as TIM23 or TIM22, can also act as receptors.[33] Therefore, it is possible that other receptors may regulate the mitochondrial morphology and biogenesis.

MAPK signaling is well characterized as being involved in cardiac hypertrophy, which is also sensitive to ROS stimuli.[8] A previous study discovered that cRaf-MEK-ERK signaling was activated by increased ROS levels in hypertrophic hearts.[11] However, our results indicated that phosphorylated JNK and P38 but not ERK1/2 were upregulated in pressure-overload–induced TIM50-deficient mice. We further

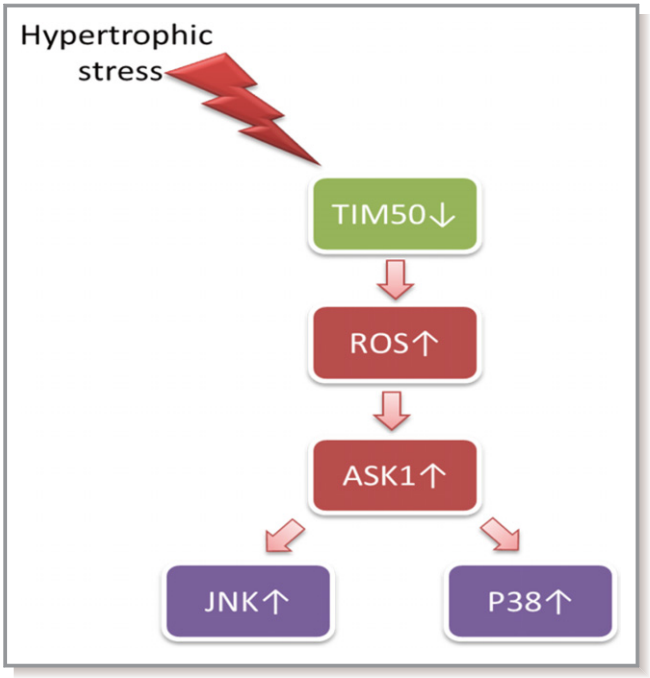

Figure 9. Schematic diagram of how TIM50 regulates cardiac hypertrophy. TIM50 is downregulated in hypertrophic hearts, which further leads to excessive ROS generation. ROS can activate ASK1, which further increases the activity of JNK and P38. ROS indicates reactive oxygen species; TIM50, translocase of the inner membrane 50.

demonstrated that ASK1, an upstream regulator of both JNK and P38, was activated along with increased ROS accumulation in TIM50 KO mice, and that TIM50 overexpression reduced p-ASK1 levels. These data suggest that TIM50 can inhibit ASK1 activity during the process of cardiac hypertrophy. We speculated that the regulation of oxidative stress may be responsible for the connection between TIM50 and ASK1 because ASK1 activation can be inhibited by SOD in Ang II–induced cardiac hypertrophy,[35] whereas excessive oxidative stress can activate ASK1.[36] Hence, we treated TIM50 KO mice with NAC to reduce oxidative stress. In accordance with the previous study, we found that p-ASK1, together with JNK and P38, was downregulated in TIM50 KO mice after NAC treatment, indicating that TIM50 inhibited ASK1 activity mainly by reducing oxidative stress. Together with the inactivation of ASK1, the hypertrophic and fibrotic phenotype was also eliminated in TIM50 KO mice after NAC treatment. These data further indicate that TIM50 attenuates pathological cardiac hypertrophy via the ROS-ASK1-JNK/P38 axis.

ASK1 has long been known to act in the regulation of pathological cardiac hypertrophy.[37,38] ASK1 deficiency significantly attenuated TAC- and Ang II–induced cardiac hypertrophy accompanied by improved cardiac function. However, using cardiac-specific ASK1 transgenic mice, Liu et al[39] demonstrated an identical hypertrophic phenotype but more

severe apoptosis compared with control mice during pressure overload. These results suggested that excessive activation of ASK1 may accelerate the progression to heart failure because cardiomyocyte apoptosis is a major contributor to heart failure.[40] Our results discovered that TIM50 knockout mice showed more aggravated pulmonary congestion along with increased p-ASK1 expression, which is consistent with our hypothesis. However, cardiomyocyte-specific TIM50 overexpression markedly postponed the progress of heart failure.

To our knowledge, this is the first time TIM50 has been identified as a novel repressor of pathological cardiac hypertrophy both in vivo and in vitro. Furthermore, we clarified that TIM50 eliminated oxidative stress, which further inhibited ASK1 activation in cardiac hypertrophy (Figure 9). Thus, TIM50 may act as a promising target for the prevention and treatment of cardiac hypertrophy and heart failure.

Acknowledgments

We thank Ding-sheng Jiang for his suggestion regarding the study design and Xue-yong Zhu, Jun Gong, Ling Huang, Yan Zhang and Ya Deng for their technical assistance.

Sources of Funding

This study was supported by grants from the National Natural Science Foundation of China (No. 81270194 to Da-chun Xu and No. 81470394 and 81270256 to Ya-wei Xu).

Disclosures

None.

References

1. Drazner MH. The progression of hypertensive heart disease. *Circulation*. 2011;123:327–334.
2. Heineke J, Molkentin JD. Regulation of cardiac hypertrophy by intracellular signalling pathways. *Nat Rev Mol Cell Biol*. 2006;7:589–600.
3. Tsutsui H, Kinugawa S, Matsushima S. Mitochondrial oxidative stress and dysfunction in myocardial remodelling. *Cardiovasc Res*. 2009;81:449–456.
4. Murphy MP. How mitochondria produce reactive oxygen species. *Biochem J*. 2009;417:1–13.
5. Nickel A, Kohlhaas M, Maack C. Mitochondrial reactive oxygen species production and elimination. *J Mol Cell Cardiol*. 2014;73:26–33.
6. Yucel D, Aydogdu S, Cehreli S, Saydam G, Canatan H, Senes M, Cigdem TB, Nebioglu S. Increased oxidative stress in dilated cardiomyopathic heart failure. *Clin Chem*. 1998;44:148–154.
7. Keith M, Geranmayegan A, Sole MJ, Kurian R, Robinson A, Omran AS, Jeejeebhoy KN. Increased oxidative stress in patients with congestive heart failure. *J Am Coll Cardiol*. 1998;31:1352–1356.
8. Tsutsui H, Kinugawa S, Matsushima S. Oxidative stress and heart failure. *Am J Physiol Heart Circ Physiol*. 2011;301:H2181–H2190.
9. Sabri A, Hughie HH, Lucchesi PA. Regulation of hypertrophic and apoptotic signaling pathways by reactive oxygen species in cardiac myocytes. *Antioxid Redox Signal*. 2003;5:731–740.
10. Wu R, Wyatt E, Chawla K, Tran M, Ghanefar M, Laakso M, Epting CL, Ardehali H. Hexokinase II knockdown results in exaggerated cardiac hypertrophy via increased ROS production. *EMBO Mol Med*. 2012;4:633–646.
11. Zhang Y, Xu J, Luo YX, An XZ, Zhang R, Liu G, Li H, Chen HZ, Liu DP. Overexpression of mitofilin in the mouse heart promotes cardiac hypertrophy in response to hypertrophic stimuli. *Antioxid Redox Signal*. 2014;21:1693–1707.
12. Ku HJ, Ahn Y, Lee JH, Park KM, Park JW. IDH2 deficiency promotes mitochondrial dysfunction and cardiac hypertrophy in mice. *Free Radic Biol Med*. 2015;80:84–92.
13. Anderson S, Bankier AT, Barrell BG, de Bruijn MH, Coulson AR, Drouin J, Eperon IC, Nierlich DP, Roe BA, Sanger F, Schreier PH, Smith AJ, Staden R, Young IG. Sequence and organization of the human mitochondrial genome. *Nature*. 1981;290:457–465.
14. Neupert W, Herrmann JM. Translocation of proteins into mitochondria. *Annu Rev Biochem*. 2007;76:723–749.
15. Balaker AE, Ishiyama P, Lopez IA, Ishiyama G, Ishiyama A. Immunocytochemical localization of the translocase of the outer mitochondrial membrane (Tom20) in the human cochlea. *Anat Rec (Hoboken)*. 2013;296:326–332.
16. Salhab M, Patani N, Jiang W, Mokbel K. High TIMM17A expression is associated with adverse pathological and clinical outcomes in human breast cancer. *Breast Cancer*. 2012;19:153–160.
17. Li J, Qi M, Li C, Shi D, Zhang D, Xie D, Yuan T, Feng J, Liu Y, Liang D, Xu X, Chen J, Xu L, Zhang H, Ye J, Lv F, Huang J, Peng L, Chen YH. TOM70 serves as a molecular switch to determine pathological cardiac hypertrophy. *Cell Res*. 2014;24:977–993.
18. Mokranjac D, Sichting M, Popov-Celeketic D, Mapa K, Gevorkyan-Airapetov L, Zohary K, Hell K, Azem A, Neupert W. Role of TIM50 in the transfer of precursor proteins from the outer to the inner membrane of mitochondria. *Mol Biol Cell*. 2009;20:1400–1407.
19. Geissler A, Chacinska A, Truscott KN, Wiedemann N, Brandner K, Sickmann A, Meyer HE, Meisinger C, Pfanner N, Rehling P. The mitochondrial presequence translocase: an essential role of TIM50 in directing preproteins to the import channel. *Cell*. 2002;111:507–518.
20. Meinecke M. TIM50 maintains the permeability barrier of the mitochondrial inner membrane. *Science*. 2006;312:1523–1526.
21. Guo Y, Cheong N, Zhang Z, De Rose R, Deng Y, Farber SA, Fernandes-Alnemri T, Alnemri ES. TIM50, a component of the mitochondrial translocator, regulates mitochondrial integrity and cell death. *J Biol Chem*. 2004;279:24813–24825.
22. Jiang X, Deng KQ, Luo Y, Jiang DS, Gao L, Zhang XF, Zhang P, Zhao GN, Zhu X, Li H. Tumor necrosis factor receptor-associated factor 3 is a positive regulator of pathological cardiac hypertrophy. *Hypertension*. 2015;66:356–367.
23. Zhu X, Fang J, Jiang D, Zhang P, Zhao G, Zhu X, Yang L, Wei X, Li H. Exacerbating pressure overload-induced cardiac hypertrophy: novel role of adaptor molecule Src homology 2-B3. *Hypertension*. 2015;66:571–581.
24. Zhao YF, Xu DC, Zhu GF, Zhu MY, Tang K, Li WM, Xu YW. Growth arrest-specific 6 exacerbates pressure overload-induced cardiac hypertrophy. *Hypertension*. 2015;67:118–129.
25. Mookerjee A, Basu JM, Majumder S, Chatterjee S, Panda GS, Dutta P, Pal S, Mukherjee P, Efferth T, Roy S, Choudhuri SK. A novel copper complex induces ROS generation in doxorubicin resistant Ehrlich ascites carcinoma cells and increases activity of antioxidant enzymes in vital organs in vivo. *BMC Cancer*. 2006;6:267.
26. Huang Q, Zhou HJ, Zhang H, Huang Y, Hinojosa-Kirschenbaum F, Fan P, Yao L, Belardinelli L, Tellides G, Giordano FJ, Budas GR, Min W. Thioredoxin-2 inhibits mitochondrial reactive oxygen species generation and apoptosis stress kinase-1 activity to maintain cardiac function. *Circulation*. 2015;131:1082–1097.
27. Takimoto E, Kass DA. Role of oxidative stress in cardiac hypertrophy and remodeling. *Hypertension*. 2007;49:241–248.
28. Santos CX, Anilkumar N, Zhang M, Brewer AC, Shah AM. Redox signaling in cardiac myocytes. *Free Radic Biol Med*. 2011;50:777–793.
29. Maulik SK, Kumar S. Oxidative stress and cardiac hypertrophy: a review. *Toxicol Mech Methods*. 2012;22:359–366.
30. Dai DF, Santana LF, Vermulst M, Tomazela DM, Emond MJ, MacCoss MJ, Gollahon K, Martin GM, Loeb LA, Ladiges WC, Rabinovitch PS. Overexpression of catalase targeted to mitochondria attenuates murine cardiac aging. *Circulation*. 2009;119:2789–2797.
31. Lu Z, Xu X, Hu X, Zhu G, Zhang P, van Deel ED, French JP, Fassett JT, Oury TD, Bache RJ, Chen Y. Extracellular superoxide dismutase deficiency exacerbates pressure overload-induced left ventricular hypertrophy and dysfunction. *Hypertension*. 2008;51:19–25.
32. Alder NN, Jensen RE, Johnson AE. Fluorescence mapping of mitochondrial TIM23 complex reveals a water-facing, substrate-interacting helix surface. *Cell*. 2008;134:439–450.
33. Marin-Garcia J, Goldenthal MJ, Moe GW. Mitochondrial pathology in cardiac failure. *Cardiovasc Res*. 2001;49:17–26.

34. Kulawiak B, Hopker J, Gebert M, Guiard B, Wiedemann N, Gebert N. The mitochondrial protein import machinery has multiple connections to the respiratory chain. *Biochim Biophys Acta*. 2013;1827:612–626.
35. Izumiya Y, Kim S, Izumi Y, Yoshida K, Yoshiyama M, Matsuzawa A, Ichijo H, Iwao H. Apoptosis signal-regulating kinase 1 plays a pivotal role in angiotensin II-induced cardiac hypertrophy and remodeling. *Circ Res*. 2003;93:874–883.
36. Soga M, Matsuzawa A, Ichijo H. Oxidative stress-induced diseases via the ASK1 signaling pathway. *Int J Cell Biol*. 2012;2012:439587.
37. Yamashita T, Yamamoto E, Kataoka K, Nakamura T, Matsuba S, Tokutomi Y, Dong YF, Ichijo H, Ogawa H, Kim-Mitsuyama S. Apoptosis signal-regulating kinase-1 is involved in vascular endothelial and cardiac remodeling caused by nitric oxide deficiency. *Hypertension*. 2007;50:519–524.
38. Nako H, Kataoka K, Koibuchi N, Dong YF, Toyama K, Yamamoto E, Yasuda O, Ichijo H, Ogawa H, Kim-Mitsuyama S. Novel mechanism of angiotensin II-induced cardiac injury in hypertensive rats: the critical role of ASK1 and VEGF. *Hypertens Res*. 2012;35:194–200.
39. Liu Q, Sargent MA, York AJ, Molkentin JD. ASK1 regulates cardiomyocyte death but not hypertrophy in transgenic mice. *Circ Res*. 2009;105:1110–1117.
40. van Empel VP, Bertrand AT, Hofstra L, Crijns HJ, Doevendans PA, De Windt LJ. Myocyte apoptosis in heart failure. *Cardiovasc Res*. 2005;67:21–29.

Supplemental Material

Figure S1

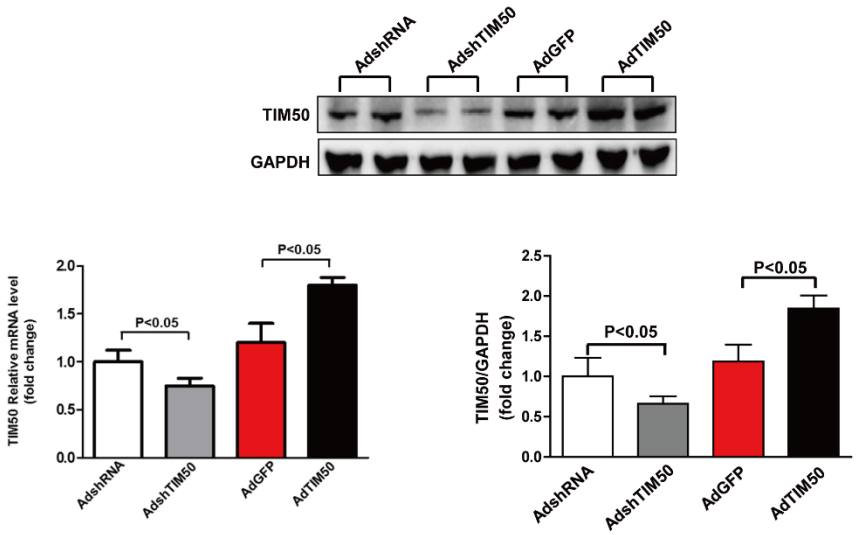

Figure S1. The mRNA and protein level of TIM50 after treatment of AdshRNA, AdshTIM50, AdGFP and AdTIM50 (n=4 independent experiments) (AdGFP: adenoviral vectors containing the green fluorescent protein gene; AdshRNA: adenoviral vectors containing the scramble shRNA sequence; AdshTIM50: adenoviral vectors containing the TIM50 shRNA sequence; AdTIM50: adenoviral vectors containing the TIM50 cDNA)

Figure S2

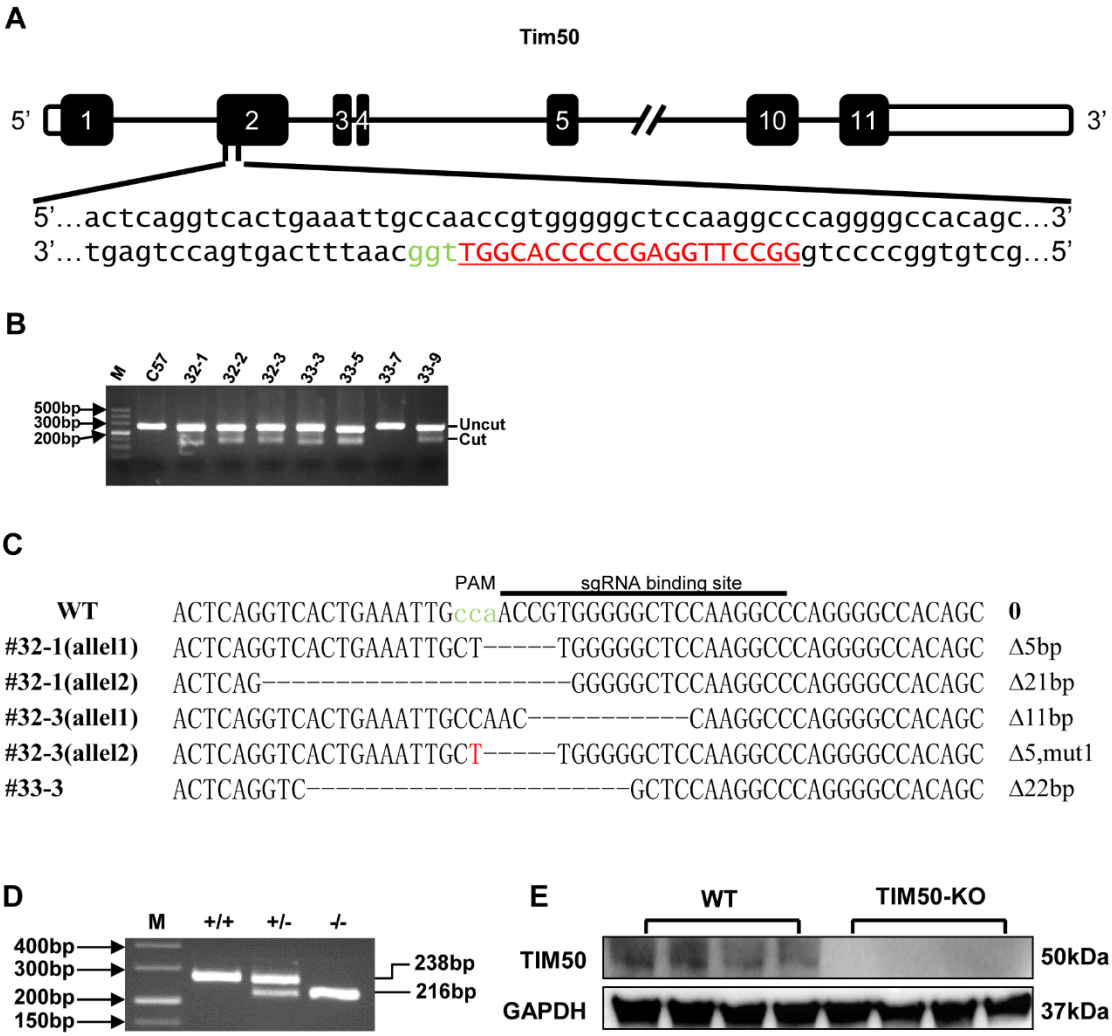

Figure S2. Schematic diagram of the generation of TIM50 KO mice. **A**, Single guiding RNA was designed and construct to target exon 2 of TIM50 gene **B**, T7E1 assay indicated 6 samples have cleavage products (32-1; 32-2; 32-3; 33-3; 32-5; 33-9), suggesting a mutant in these transgenic mouse line. **C**, Sequence analysis of these mutants in mice **D**, we selected 33-3 mouse line to perform the next experiments. PCR analysis was performed to detect the gene mutation of wild type mice, heterozygous F1 offspring and the homozygous F2 offspring. **E**, Representative Western blot results to confirm the protein expression of TIM50 in the hearts of WT and knockout mice (n=4 per experimental group).

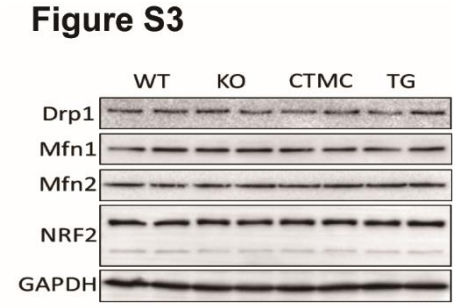

Figure S3. The expression of mitochondrial morphology and biogenesis-related proteins.